Chin. Sci. Bull. (2014) 59(18):2214–2220
DOI 10.1007/s11434-014-0243-4

csb.scichina.com
www.springer.com/scp

Article

Materials Science

Polarization behavior of microbial fuel cells under stack operation

Zejie Wang · Yicheng Wu · Lu Wang · Feng Zhao

Received: 31 July 2013 / Accepted: 18 October 2013 / Published online: 26 March 2014

Abstract The polarization behavior of microbial fuel cells (MFCs) was evaluated under different stack operation modes, including series, parallel, series–parallel, and parallel–series. During the stack operation, voltages of individual MFCs, subunit stacks, and overall stacks were recorded as a function of the current. Meanwhile, the potentials of individual MFCs' anode and cathode were also determined via Ag/AgCl electrodes to study the change in potentials under stack operations. The results demonstrated that the MFCs with relatively low ability to generate current were easier to suffer polarity reversal in the series stack, which was confirmed in the series subunit of the series–parallel stack. MFCs with high electroactivity would be enhanced to generate larger maximum power; however, MFCs with low electroactivity outputted smaller maximum power in a parallel stack. The changes in individual MFCs' behavior under stack operation mode were determined primarily caused by the influences on the behavior of the anode. Results of the present study provide valuable information for optimization of stack operation of MFCs.

Keywords Microbial fuel cells · Stack operation · Polarization · Power generation

SPECIAL ISSUE: Advanced Materials for Clean Energy

Electronic supplementary material The online version of this article (doi:10.1007/s11434-014-0243-4) contains supplementary material, which is available to authorized users.

Z. Wang · Y. Wu · L. Wang · F. Zhao (✉)
Institute of Urban Environment, Chinese Academy of Sciences, Xiamen 361021, China
e-mail: fzhao@iue.ac.cn

1 Introduction

Increasing development in economy and society consumes large amount of fossil fuels and leads to serious environmental pollution. Great efforts are devoted to the development of novel energy sources, such as solar energy, wind power, and biofuel. Among those, microbial fuel cells (MFCs) present great potential to contribute to the reduction of the use of fossil fuels in virtue of its ability to output electric power from feedstocks containing large quantities of organic substrates, and to efficiently remove both organic and inorganic contaminants through the activity of micro-organism that colonizes the anode [1–6].

Power density yields in MFCs have increased 5–6 orders of magnitude over the last decade as a result of the optimization of reactor configuration, the improvement of operational parameters, the selection of bacteria with greater electrochemical activity, and the application of novel electrode materials [7–10]. However, bottlenecks for the practical application of MFC are still present. For instance, the theoretical voltage output is only 1.1 V when oxygen is used as an electron acceptor and sodium acetate as an electron donor. Furthermore, the practical voltage output of MFCs is much lower than the theoretical value, due to electrochemical phenomena such as charge transfer overpotential, ohmic overpotential, and mass transport overpotential [11]. Therefore, stacking multiple MFCs is a promising strategy to achieve enhanced output of voltage and current for practical application of MFC technology [12–19]. In previous reports on stack operation of MFCs, individual MFCs were linked in series for higher voltage output, in parallel to generate larger current, or in series–parallel as a trade-off approach to increase both voltage and current output. Despite the enhanced voltage and current output for series and parallel stack respectively, well matched voltage and current are

needed if the MFC stack is to be adopted to directly drive electronics in practical applications. Therefore, the series–parallel stack mode, as an alternative to series and parallel stacks, was evaluated as a possible approach to enhance the output of both voltage and current [14]. As the elementary unit of stack, the polarization behavior of individual MFCs would be affected during stack operation mode, affecting the performance of the stack; therefore, understanding the polarization behavior of individual MFCs is essential to optimize the performance of MFC stacks. However, there is no overall and detailed information on this aspect, especially on how the electrode potential changed after the MFCs were connected in stacks [12, 17].

In this study, multiple individual MFCs were connected in different stack modes of series, parallel, series–parallel (S–P), and parallel–series (P–S). During the stack operation, the voltage, electrode potential, and internal resistance of individual MFCs were assessed to observe the effect of stack operation on the polarization behavior of individual MFCs. The results of the present study provide valuable information for the optimization of stack operation of MFCs.

2 Materials and methods

2.1 MFC and inoculation

The two-chambered MFC reactors used in this study were constructed of Plexi-glass, with the anodic and cathodic chambers separated by a cation exchange membrane (Zhejiang Qianqiu Group Co. Ltd., China). Each chamber has a size of 137.5 mL ($(5.5 \times 5 \times 5)$ cm^3), with a working volume of 125 mL. Both anode and cathode were prepared from graphite felt (Haoshi Carbon Fiber Co. Ltd., China), with projected surface area of 16 cm^2 ((4×4) cm^2). The MFCs were inoculated with anaerobic culture collected from Jimei wastewater treatment plant at different time and adopted different species of electron acceptors of O_2, $KMnO_4$, and $K_3[Fe(CN)_6]$. For the stack operation mode, the anode chambers were filled with 125 mL artificial wastewater containing (g/L) sodium acetate, 4.1 (equivalent to 50.0 mmol/L); KH_2PO_4, 6.28; K_2HPO_4, 10.0; $NaHCO_3$, 2.0; NaCl, 0.5; Na_2SO_4, 0.5; $MgSO_4{\cdot}7H_2O$, 0.2. The cathode chambers were filled with 125 mL buffer solution (pH 6) containing $Na_2HPO_4{\cdot}12H_2O$, 8.81 g/L; $NaH_2PO_4{\cdot}2H_2O$, 41.05 g/L; and $K_3[Fe(CN)_6]$, 100 mmol/L as electron acceptor. The MFCs were operated in fed-batch mode. Both anolyte and catholyte were replaced with fresh ones after one or two cycles operation.

2.2 Stack operation and analysis

Stack operation was achieved by linking MFC reactors in series, parallel, series–parallel, and parallel–series, connecting the anode of one cell to the cathode of another cell with titanium wire. The polarization curves were obtained by changing the external resistance from 10 kΩ to 25 Ω, (except for the parallel stack operation, which was performed by changing from 10 kΩ to 10 Ω) using a fuel cell test system (Maccor Inc., USA). From the polarization curves, the maximum power (P_{max}) is determined. The voltage (V_{cell}) of individual MFCs and subunits, and the anode potential (P_a) were recorded as auxiliary voltage. Current (i) was recorded with a multimeter (Keithley Instruments Inc., USA). The cathode potential (P_c) was calculated as $P_c = V_{cell} + P_a$. Electric power (P) was determined as $P = V_{cell} \cdot i$. Internal resistance (R_{int}) was determined as the slope of the i-V_{cell} curve, according to $V_{cell} = U_{cell} - iR_{int}$, where U_{cell} is the electromotive force of the cell [20]. The experiments were carried out at a temperature of (27 ± 1) °C.

3 Results and discussion

3.1 Performance of individual MFCs

To determine the change in MFCs' polarization behavior under stack operation, the polarization behavior of individual MFCs was first analyzed as a comparison by varying the external resistance from 10 kΩ to 25 Ω with the aid of a battery test system. Figure 1 shows the polarization behaviors of the six individual MFCs (labeled C1–C6). The maximum power output for C1–C6 was 1.55, 1.05, 1.27, 1.14, 0.84, and 0.55 mW, at currents of 3.92, 2.28, 2.51, 2.37, 1.45, and 0.96 mA, respectively (Fig. 1a; Table 1). Therefore, the ability to generate electric power of the six individual MFCs can be ranked as C1 > C3 > C4 > C2 > C5 > C6. The R_{int} of C1–C6 was determined as 68.09, 102.90, 89.50, 105.00, 107.00, and 164.59 Ω, respectively (Table 1). The voltages of individual MFCs are similar at low currents; however, as current increased, differences in voltage were observed (Fig. 1b). The polarization curves of C2, C3, and C4 displayed a slight overshoot, in correspondence with the behavior of the anode, while the cathodic potential showed no significant differences (Fig. 1c). The results demonstrate that the difference in individual MFCs polarization behavior is dependent on the anodes' performance.

In this study, different electron acceptors were used to establish the MFCs, and different currents were generated during the startup period (data not shown), which was probably the reason for the different performances of the individual MFCs. In stack operation, differences in individual MFC's performance would unavoidably occur. Therefore, the use in this study of individual MFCs with different performances in stack operation makes it easier to discover problems that may arise during the practical application of MFC stacks.

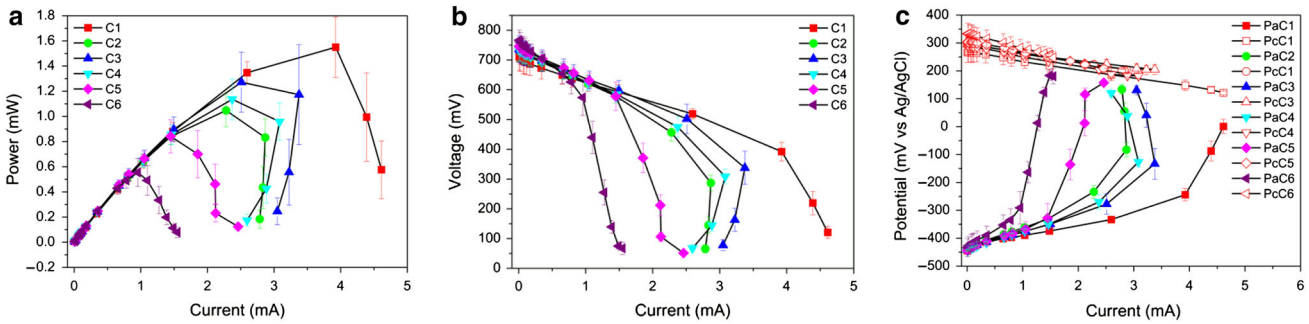

Fig. 1 (Color online) Performance of individual MFCs: power output (**a**), voltage (**b**), and electrode potential (**c**) as a function of current

3.2 Stack operation

3.2.1 Series stack

Linking multiple individual MFCs in series is an efficient way of achieving high-voltage output, and in theory, the voltage output from the series stack should be the sum of the voltage outputs of the individual MFCs. By linking 6 individual MFC in series, the maximum power observed was 4.02 mW at a current of 1.41 mA (Fig. 2a). This P_{max} is smaller than the sum of P_{max} (5.56 mW) generated by MFCs running individually. The P_{max} of C5 and C6 was 0.69 and 0.21 mW, respectively, but with a large standard error (Fig. 2a; Table 1). Furthermore, the polarization behavior of C1–C4 was significantly affected despite the P_{max} did not clearly change compared to individual operation (Fig. S1 online). Compared to individually operated MFCs, the R_{int} of C5 increased from 107.00 to 206.30 Ω, and that of C6 increased from 164.59 to 652.50 Ω (Table 1). The polarization curves of C5 and C6 showed reversal polarization (Fig. 2a), attributable to the performance of the anode, which reached a potential higher than 1,000 mV (Fig. 2c). Voltage reversal of C5 and C6 occurred when the current reached 2.65 and 1.41 mA, respectively (Fig. 2b), probably due to their lower electroactivity.

Voltage reversal is a common phenomenon during series stack operation when the potential of the anode becomes higher than that of the cathode. Voltage reversal can deteriorate the electroactive ability of the micro-organisms, increasing the R_{int}, and further reducing the electric power output of the stack. In this study, the performance of C6 did not recover to the level of electric power output due to the effect of voltage reversal over two cycles. Aelterman et al. [16] first reported MFC voltage reversal in series stack operation, and fuel starvation and the catalytic property of the biofilm were considered as the causes of this phenomenon. Oh et al. [12] confirmed the contribution of fuel starvation to voltage reversal by limiting fuel supply to one of the cells in a two-cell series stack. Organic matter removal is positively related to the current generated from a MFC [21]. Since the same concentration of initial substrate is supplied to the individual MFCs in the series stack, fuel starvation, should it occur, would be first observed in the MFCs with higher ability to generate current. However, voltage reversal occurred to MFCs with lower electroactivity (C5 and C6 in this study). This suggests that voltage reversal would occur first to MFCs with lower ability to generate current compared to the others in a series stack. Therefore, MFCs with similar individual performances are a requisite for optimal series stack operation.

3.2.2 Parallel stack

Stack operation in parallel could increase the generation of current due to the reduction of the overall R_{int}. Since C6 was not able to recover the performance shown before voltage reversal, five individual MFCs (C1–C5) were connected in parallel. A P_{max} of 6.84 mW was generated at a current of 16.49 mA for the parallel stack. The overall R_{int} was 20.40 Ω. For C1, the MFC with largest output power, the P_{max} increased to 1.92 from 1.55 mW, the value observed during individual activity; however, the P_{max} for C5 was limited to 0.32 mW compared to 0.84 mW in individual operation, due to the change in R_{int} from 107.00 to 543.96 Ω (Fig. 3a; Table 1). The anode performance of C1 was enhanced while that of C5 was limited in comparison to that of C1 and C5 during individual operation (Fig. 3b).

Individual MFCs in a parallel stack operation present all the same voltage, while the current of the stack is the sum of that of the individual MFCs. Therefore, MFCs with relatively small internal resistance will generate higher current and contribute more to the total current of the parallel stack. In a parallel stack, electrons generated at anode are collected and flow through the external circuit to the cathodes. During this process, electrons tend to flow to the cathode of the MFCs with relatively small R_{int}. In order to keep electric neutrality, more electrons need to be generated at the anode of the MFCs with higher electroactivity, while fewer electrons would be generated at the anode of MFCs with lower

Table 1 Performance of individual MFCs and overall stacks in terms of P_{max}, i-P_{max}, and R_{int} in the different MFC systems

	P_{max} (mW)					i-P_{max} (mA)				
	Individual	Series	Parallel	S–P	P–S	Individual	Series	Parallel	S–P	P–S
C1	1.55 ± 0.24	1.58 ± 0.07	1.92 ± 0.06	1.37 ± 0.23	1.92 ± 0.12	3.92 ± 0.31	2.78 ± 0.02	4.58 ± 0.14	3.37 ± 0.53	4.71 ± 0.07
C2	1.05 ± 0.13	1.14 ± 0.12	1.15 ± 0.05	0.71 ± 0.32	1.16 ± 0.08	2.23 ± 0.14	2.65 ± 0.11	2.74 ± 0.09	1.85 ± 0.87	2.84 ± 0.14
C3	1.27 ± 0.24	1.51 ± 0.07	1.64 ± 0.03	1.37 ± 0.07	1.26 ± 0.13	2.51 ± 0.25	2.78 ± 0.02	3.95 ± 0.06	2.87 ± 0.28	2.39 ± 0.21
C4	1.14 ± 0.16	1.32 ± 0.05	1.13 ± 0.02	1.22 ± 0.09	0.93 ± 0.07	2.37 ± 0.18	2.65 ± 0.11	2.69 ± 0.01	2.87 ± 0.28	1.76 ± 0.12
C5	0.84 ± 0.13	0.69 ± 0.31	0.32 ± 0.00	0.63 ± 0.10	0.34 ± 0.07	1.45 ± 0.12	1.41 ± 0.18	1.50 ± 0.01	2.24 ± 0.52	0.99 ± 0.18
C6	0.55 ± 0.11	0.21 ± 0.42	–	–	–	0.96 ± 0.10	0.87 ± 0.11	–	–	–
C1C2	–	–	–	1.74 ± 0.31	3.08 ± 0.20	–	–	–	2.88 ± 0.55	7.48 ± 0.66
C3C4C5	–	–	–	3.06 ± 0.36	2.69 ± 0.41	–	–	–	2.49 ± 0.39	5.19 ± 0.18
Overall	–	4.02 ± 1.01	6.84 ± 0.24	4.58 ± 0.30	5.64 ± 0.96	–	1.41 ± 0.18	16.50 ± 0.33	4.78 ± 0.16	7.48 ± 0.66

	R_{int} (Ω)				
	Individual	Series	Parallel	S–P	P–S
C1	68.09 ± 10.61	63.15 ± 11.71	71.46 ± 2.23	104.38 ± 5.31	66.88 ± 5.43
C2	102.90 ± 24.9	113.90 ± 20.45	125.58 ± 3.91	217.18 ± 11.71	115.52 ± 9.38
C3	89.50 ± 21.95	74.00 ± 9.19	84.20 ± 2.69	70.80 ± 12.31	89.72 ± 14.14
C4	105.00 ± 13.40	94.78 ± 12.03	117.36 ± 6.49	90.17 ± 9.02	123.93 ± 19.54
C5	107.00 ± 18.72	206.30 ± 49.42	543.96 ± 51.41	217.76 ± 21.54	282.56 ± 48.37
C6	164.59 ± 48.42	652.50 ± 209.26	–	–	–
C1C2	–	–	–	330.78 ± 22.64	43.15 ± 3.51
C3C4C5	–	–	–	373.53 ± 44.92	43.22 ± 6.81
Overall	–	1305.40 ± 23.22	20.40 ± 0.65	172.67 ± 17.70	84.59 ± 11.25

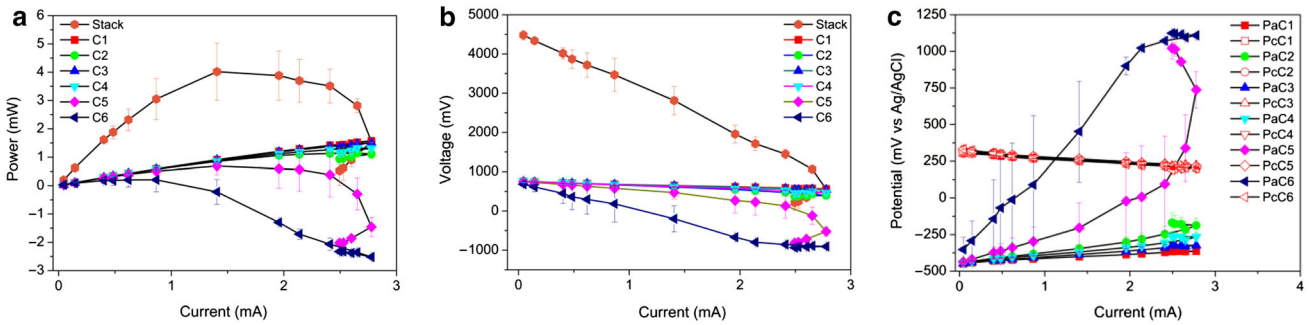

Fig. 2 (Color online) Power output (**a**) and voltage (**b**) of overall stack and individual MFCs, and electrode potential (**c**) in series stack operation

electroactivity. This may explain why the anodic performance of C1 was enhanced, while that of the C5 was reduced.

3.2.3 Series–parallel stack

As a trade-off of series and parallel stacks, the S–P stack was demonstrated to be efficient to promote both the voltage and current output of the stack in comparison to series and parallel stacks. The change in polarization behavior of individual MFCs in the stack of S–P was also evaluated in this study. To achieve a S–P stack, cells of C1 and C2 were linked in a series (C1C2), and then connected in parallel with another series stack of C3, C4, and C5 (C3C4C5).

From the polarization curves shown in Fig. 4a, a P_{max} of 4.58 mW was generated from the overall stack at a current of 4.78 mA. The P_{max} for the series subunit of C1C2 and C3C4C5 was 1.74 and 3.06 mW, at currents of 2.88 and 2.49 mA, respectively (Table 1). In the C1C2 subunit, the P_{max} of C2 was reduced to 0.71 from the individual opeartion value of 1.05 mW; in the C3C4C5 subunit, the P_{max} of C5 was decreased to 0.63 mW in comparison to the individual operation value of 0.84 mW (Table 1). For both C2 and C5, the MFCs with relatively lower electroability in the subunits of C1C2 and C3C4C5, voltage reversal occurred as the current increased to 3.37 and 2.87 mA, respectively, corresponding to an increase in anodic potential (Fig. 4b, c). The voltage of C1 and C2 largely fluctuated at higher resistances (Fig. 4b), which is in line with the variation of the anodic potentials of C1 and C2 (Fig. 4c).

In a S–P stack, the series subunits showed the same voltage, while different currents were observed depending on the electrochemical characteristics, such as the internal resistance of the subunit. Due to different number of MFCs in the two series subunits, the open circuit voltage of the C3C4C5 subunit was larger than that of the C1C2 subunit. Therefore, C1 and C2 were forced to adjust their voltage to achieve an equal overall voltage to that of the C3C4C5 subunit, resulting in fluctuation in cell voltage at large resistances. The potential of a chemical electron acceptor (in this case $K_3[Fe(CN)_6]$) depends on its concentration and the pH of the solution, according to Nernst equation; therefore, it is difficult to adjust the cathodic potential once the concentration of the electron acceptor and the pH of the catholyte are fixed. This means that the C1C2 subunit has to adjust the voltage through changes in the anodic potential rather than the cathodic potential to equalize the voltage with the C3C4C5 subunit. The mechanism by which C1 and C2 adjust their anodic potential may be through changes in the potential of the proteins involved in electron transfer by electroactive micro-organisms.

C2 and C5, with a relatively low ability to output electric power compared to the other cell(s) in C1C2 and C3C4C5 series subunit, suffered voltage reversal. As the results showed for the series stack, C2 did not show voltage reversal, contrary to what was observed in the series subunit C1C2 of the S–P stack. Therefore, the results support the conclusion that individual MFCs with relatively lower ability to generate electric power in a series stack were vulnerable to suffer voltage reversal.

3.2.4 Parallel–series stack

As it was mentioned earlier, P–S stack is a trade-off alternative to parallel and series stack. However, no studies have been reported of power generation through P–S stack of MFCs. To get a P–S stack in this study, individual cells of C1 and C2 (C1C2), and C3, C4, and C5 (C3C4C5) were connected in parallel, and then the parallel subunits of C1C2 and C3C4C5 were connected in series. The P_{max} for the P–S stack was determined to be 5.64 mW at a current of 7.48 mA, corresponding to a P_{max} of 3.08 mW for the subunit of C1C2, and a P_{max} of 2.69 mW for the subunit of C3C4C5, respectively (Fig. 5a). The R_{int} of the overall stack, the C1C2 subunit, and the C3C4C5 subunit were 84.59, 43.15, and 43.22 Ω, respectively (Table 1). The voltage of the subunits of C1C2 and C3C4C5 reversed alternately at high current, but did not result in voltage reversal of the overall stack (Fig. 5b). The P_{max} for C1 in the stack was 1.92 mW compared to an individual operation value of 1.55 mW, while the P_{max} of C5 was reduced

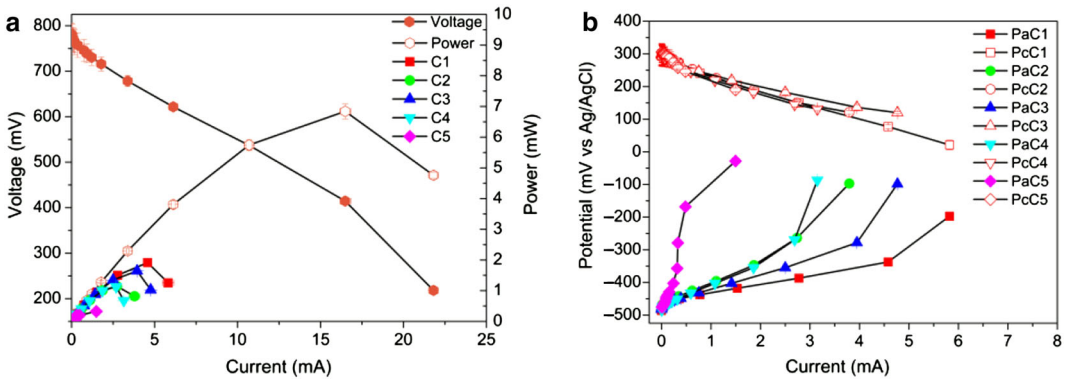

Fig. 3 (Color online) Voltage and power of the overall parallel stack and individual MFCs (**a**), and electrode potential of individual MFCs (**b**)

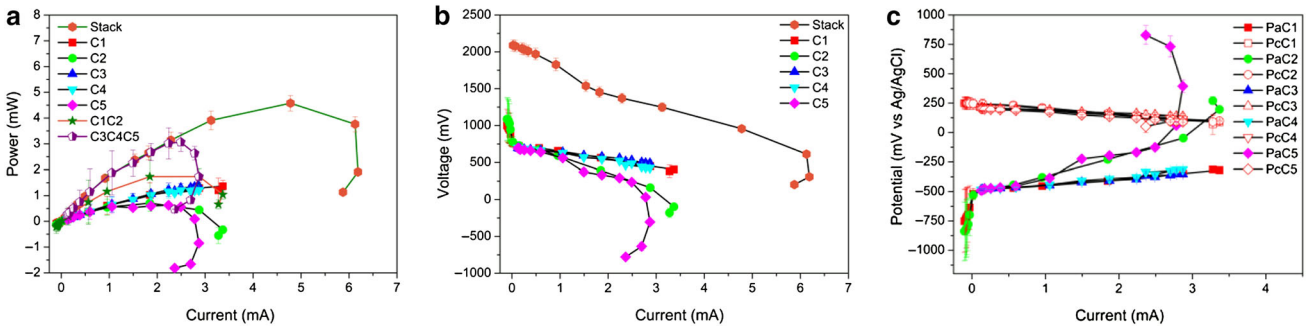

Fig. 4 (Color online) Performance of series–parallel stack and individual MFCs: power (**a**), voltage (**b**), and electrode potential (**c**)

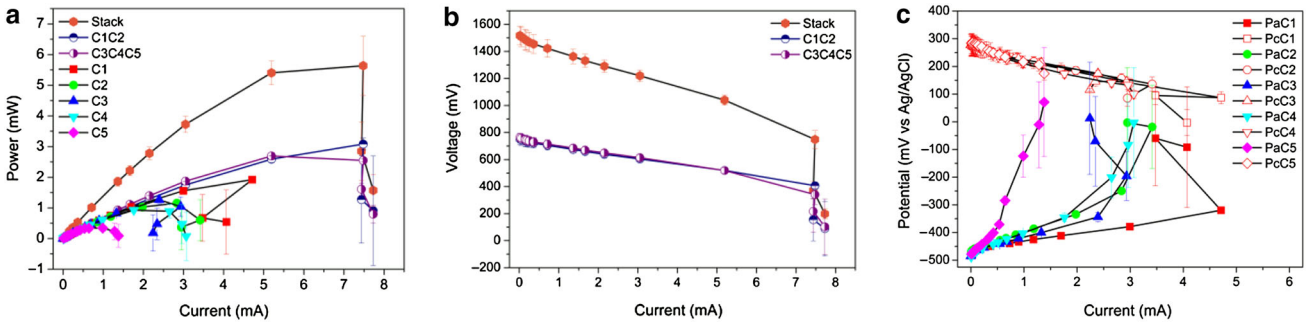

Fig. 5 (Color online) Power (**a**), voltage (**b**), and electrode potential (**c**) of overall parallel–series stack and individual MFCs

from 0.84 to 0.34 mW under stack operation. Under P–S stack operation, the anodic potential of all the individual MFCs significantly fluctuated at high current (Fig. 5c).

As a hybrid of parallel and series stack, the P–S stack possesses the electrochemical characteristics of both parallel stack and series stack, but it eventually affected the characteristics of a series stack. In P–S stack, the same current flowed across the parallel subunits of C1C2 and C3C4C5; thereby, the parallel subunits affected each other to achieve an equal current. As cells with relatively higher ability to generate electric power in the parallel stack of C1C2 and C3C4C5, the polarization curves of C1 and C3 showed an overshoot, caused by the performance of the anodes. This was possibly caused by cells in each parallel subunit sharing equal voltage, while the sum of current flowing across the cells of C1 and C2 should be equal to that of C3, C4, and C5; therefore, cells with higher ability to generate current were more affected. In parallel subunits, the P_{max} of C1 was enhanced, while that of C5 was reduced, both in comparison to that of individual operation. This phenomenon was in line with that observed in the parallel stack.

In addition to the effect of parallel stack, individual MFCs were indirectly influenced by the characteristics of

the series stack. The subunits of C1C2 and C3C4C5 in the present study suffered voltage reversal alternately, which further resulted in the anodic potential fluctuation of all individual MFCs at high current.

4 Conclusions

Individual MFCs in a series stack with relatively lower ability to generate current than the other MFCs in the system are more susceptible to suffer polarity reversal; and MFCs not suffering polarity reversal in a series stack are liable to show polarity reversal in the series subunit of a series–parallel stack, as long as the MFCs have lower electroactivity compared to the other MFCs in the same series subunit. To avoid polarity reversal of MFCs in a series stack, MFCs with similar performance should be used. Parallel stack mode enhances the maximum power of MFCs with high electroability, while limit the maximum power of MFCs with low electroability. Parallel subunits in parallel–series stack would suffer polarity reversal at high current; however, the polarity reversal occurs alternately and thus does not result in voltage reversal of the overall stack. In parallel–series stack, all the MFCs' anodic potentials suffer significant fluctuation due to the voltage reversal of the subunits.

Acknowledgments This work was supported by the Main Direction Program of Knowledge Innovation (KZCXZ-EW-402), the Hundred Talents Program of the Chinese Academy of Sciences, the National Natural Science Foundation of China (21177122, 21306182), and Ministry of Science and Technology (2011AA060907). Thanks should be given to Dr. Claudio Avignone-Rossa from University of Surry, UK for the English edition and helpful suggestions.

References

1. Zhao F, Rahunen N, Varcoe JR et al (2009) Factors affecting the performance of microbial fuel cells for sulfur pollutants removal. Biosens Bioelectron 24:1931–1936
2. Wang Z, Lim B, Lu H et al (2010) Cathodic reduction of Cu^{2+} and electric power generation using a microbial fuel cell. Bull Korean Chem Soc 31:2025–2030
3. Wang Z, Lim B, Choi C (2011) Removal of Hg^{2+} as an electron acceptor coupled with power generation. Bioresour Technol 102:6304–6307
4. Zhang BG, Zhou SG, Zhao HZ et al (2010) Factors affecting the performance of microbial fuel cells for sulfide and vanadium (V) treatment. Bioprocess Biosyst Eng 33:187–194
5. Velvizhi G, Venkata Mohan S (2012) Electrogenic activity and electron losses under increasing organic load of recalcitrant pharmaceutical wastewater. Int J Hydrogen Energy 37:5969–5978
6. Lee CY, Ho KL, Lee DJ et al (2012) Electricity harvest from wastewaters using microbial fuel cell with sulfide as sole electron donor. Int J Hydrogen Energy 37:15787–15791
7. Wei J, Liang P, Huang X (2011) Recent progress in electrodes for microbial fuel cells. Bioresour Technol 102:9335–9344
8. Cheng S, Logan BE (2011) Increasing power generation for scaling up single-chamber air cathode microbial fuel cells. Bioresour Technol 102:4468–4473
9. Yi H, Nevin KP, Kim BC et al (2009) Selection of a variant of Geobacter sulfurreducens with enhanced capacity for current production in microbial fuel cells. Biosens Bioelectron 24:3498–3503
10. Fan YZ, Hu HQ, Liu H (2007) Enhanced coulombic efficiency and power density of air-cathode microbial fuel cells with an improved cell configuration. J Power Sources 171:348–354
11. Zhao F, Slade RCT, Varcoe JR (2009) Techniques for the study and development of microbial fuel cells: an electrochemical perspective. Chem Soc Rev 38:1926–1939
12. Oh S, Logan BE (2007) Voltage reversal during microbial fuel cell stack operation. J Power Sources 167:11–17
13. Shin SH, Choi YJ, Na SH et al (2006) Development of bipolar plate stack type microbial fuel cells. Bull Korean Chem Soc 27:281–285
14. Ieropoulos I, Greenman J, Melhuish C (2008) Microbial fuel cells based on carbon veil electrodes: stack configuration and scalability. Int J Energy Res 32:1228–1240
15. Ieropoulos I, Greenman J, Melhuish C (2010) Improved energy output levels from small-scale microbial fuel cells. Bioelectrochemistry 78:44–50
16. Aelterman P, Rabaey K, Pham HT et al (2006) Continuous electricity generation at high voltages and currents using stacked microbial fuel cells. Environ Sci Technol 40:3388–3394
17. Dekker A, Ter Heijne A, Saakes M et al (2009) Analysis and improvement of a scaled-up and stacked microbial fuel cell. Environ Sci Technol 43:9038–9042
18. Zhuang L, Zheng Y, Zhou S et al (2012) Scalable microbial fuel cell (MFC) stack for continuous real wastewater treatment. Bioresour Technol 106:82–88
19. Zhuang L, Yuan Y, Wang Y et al (2012) Long-term evaluation of a 10-liter serpentine-type microbial fuel cell stack treating brewery wastewater. Bioresour Technol 123:406–412
20. Liu HC, Chen SA, Logan BE (2005) Power generation in fed-batch microbial fuel cells as a function of ionic strength. Environ Sci Technol 39:5488–5493
21. Katuri KP, Scott K, Head IM et al (2011) Microbial fuel cells meet with external resistance. Bioresour Technol 102:2758–2766